**Climate
of the Past**
Open Access
Discussions

The impacts of Meltwater Pulse-1A in the South Atlantic Ocean deep circulation since the Last Glacial Maximum

J. M. Marson[1], I. Wainer[1], Z. Liu[2], and M. M. Mata[3]

[1]Oceanographic Institute, University of São Paulo, São Paulo, SP, Brazil
[3]Institute of Oceanography, Federal University of Rio Grande-FURG, Rio Grande, RS, Brazil
[2]Center for Climatic Research and Department of Atmospheric and Oceanic Sciences, University of Wisconsin, Madison, USA

Correspondence to: I. Wainer (wainer@usp.br)

Title Page

Abstract	Introduction
Conclusions	References
Tables	Figures

◄ | ►|

◄ | ►

Back | Close

Full Screen / Esc

Printer-friendly Version

Interactive Discussion

South Atlantic Ocean deep circulation

J. M. Marson et al.

Full Screen / Esc

Printer-friendly Version

Interactive Discussion

Abstract

Since 21 000 yr ago, the oceans have received large amounts of freshwater in pulses coming from the melting ice sheets. A specific event, known as meltwater pulse 1A (MWP-1A), has been identified in sea-level and temperature proxy records as respon-
sible for the increase of ∼ 20 m in sea level in less than 500 yr. Although its origin and timing are still under discussion, MWP-1A seems to have had a significant impact on several components of the climatic system. The present work aims to elucidate these impacts on the water mass distribution of the South Atlantic Ocean through the analy-sis of a transient simulation of the climate evolution from the Last Glacial Maximum to
Present Day using a state-of-art CGCM, the National Center for Atmospheric Research Community Climate System Model version 3 (NCAR CCSM3). Results show that the freshwater discharge associated with the timing of MWP-1A was crucial to establish the present thermohaline structure associated with the North Atlantic Deep Water, mark-ing the transition between a shallower and a deeper Atlantic Meridional Overturning
Circulation.

1 Introduction

The last deglaciation, triggered by increasing summer insolation in the Northern Hemi-sphere (NH) nearly 21 thousand years ago (ka), was marked by several meltwater discharge episodes resulting from ice sheet retraction. A major meltwater discharge
registered on sea level records (Fairbanks, 1989; Deschamps et al., 2012) occurred around 14 ka resulting from massive loss of ice from the ice sheets into the ocean (Weaver et al., 2003; Peltier and Fairbanks, 2006; Hanebuth et al., 2009), which was responsible for ∼ 20 m of sea level rise in less than 500 yr. This event is known as meltwater pulse 1A (MWP-1A).
   The origins of MWP-1A has been discussed in the last decades and is still subject of controversial debate. Much of the controversy surrounding the origin of MWP-1A is

related to its Northern Hemisphere source. It is suggested by several authors that this freshwater input came solely from the Laurentide Ice Sheet (LIS) over North America, ruling out any contribution from the Southern Hemisphere (SH) (Fairbanks, 1989; Peltier, 1994, 2005; Peltier and Fairbanks, 2006; Bentley et al., 2010; Mackintosh et al.,
5 2011; Anderson et al., 2013). On the other hand, several studies support the idea of a significant freshwater contribution from the Antarctic Ice Sheet (AIS) (Clark et al., 1996, 2002; Kienast et al., 2003; Weaver et al., 2003; McManus et al., 2004; Bassett et al., 2005, 2007; Carlson, 2009; Stenni et al., 2010; Bethke et al., 2012; Carlson et al., 2012; Deschamps et al., 2012; Gregoire et al., 2012). In fact, some of these
10 later studies discuss that the idea of MWP-1A generated only in the Northern Hemisphere would be inconsistent with proxy data evidence. MWP-1A originating only from the Northern Hemisphere would not be physically plausible due to the necessary melting rates needed to account for the sea level rise records (Clark et al., 1996; McManus et al., 2004; Stanford et al., 2006; Praetorius et al., 2008). The modeling study of Carl-
15 son et al. (2012) attributes about 37 % of the LIS mass loss contribution to MWP-1A, which suggests that a significant fraction of its origin could come from the AIS.

Seidov et al. (2001) and Weaver et al. (2003) suggested that meltwater discharges near the location of deep water formation in one hemisphere may lead to the strengthening of the ocean circulation in the other hemisphere. The main players on the lower
20 and upper limbs of the Atlantic Meridional Overturning Circulation (AMOC) are the Antarctic Bottom Water (AABW) and the North Atlantic Deep Water (NADW). So, when freshwater enters the North Atlantic, for example, the NADW formation rate decreases. In order to maintain the deep water input into the world ocean, more AABW is produced, which would lead to a shallower AMOC in the North Atlantic. This scenario is
25 what is believed to have happened at the Last Glacial Maximum (LGM, ~ 21 ka) when the deep Atlantic was flooded with extremely salty AABW (Marchitto et al., 2002; Curry and Oppo, 2005) and the AMOC was shallower than today (Lippold et al., 2012; Zhang et al., 2012). According to chemical proxy evidence, the AABW water does fill most of the Atlantic basin and a NH-origin water, the Glacial North Atlantic Intermediate

South Atlantic Ocean deep circulation

J. M. Marson et al.

Water (GNAIW) penetrates only to the mid-depths of the Atlantic Ocean, much shallower than the NADW (Duplessy et al., 1988; Boyle and Leach, 1995; Yu et al., 1996; Curry and Oppo, 2005; Lynch-Stieglitz et al., 2006; Marchitto and Broecker, 2006). After the Younger Dryas, at ~ 11.7 ka, there is evidence of the strengthening of the NADW (Jouzel et al., 1995; Hughen et al., 1998; Weaver et al., 2003).

In this study, these aspects of Atlantic Ocean's deep circulation are evaluated within the results of a transient simulation of the last 21 000 yr, which prescribes several meltwater pulses as identified by sea level records (including a MWP-1A with 75 % of its freshwater coming from AIS). This simulation is an extension for the Holocene of the DGL-A experiment described in Liu et al. (2009). It is our hypothesis that the present day circulation pattern of the South Atlantic Ocean was established approximately at the onset of the Holocene (11 ka). Therefore we will investigate the impacts of the freshwater discharge associated with MWP1-A, assuming contributions from both Hemispheres, on the structure of the NADW in South Atlantic Ocean.

2   Data and methods

The results of a paleoclimate transient simulation using the Community Climate System Model version 3 (CCSM3) are used in this study. CCSM is a global coupled model developed by the National Center for Atmospheric Research (NCAR). The simulation experiment analyzed is referred to as TraCE-21K. It was run from 21 ka to 0 ka (He, 2011) and it is the extended version of the DGL-A experiment discussed in Liu et al. (2009). It should be noted that the model air temperature, when compared to the GISP2 ice core reconstructions (Alley, 2000) show very good agreement (Liu et al., 2009). A brief description of TraCE-21K setup is given as follows.

The oceanic component has 25 vertical levels and a spatial resolution of 3.6° longitude and variable latitude (finer resolution of $\sim 0.9°$ in the equator). Initial conditions were established from LGM simulation results from Otto-Bliesner et al. (2006) and transient concentrations of greenhouse gases (CO_2, CH_4 and N_2O) were adopted from

Joos and Spahni (2008). The coastlines and ice sheets volume variability followed ICE-5G database (Peltier, 2004).

Several meltwater schemes were tested in sensitivity experiments (He, 2011), but just the ones that resulted in similar values compared to proxy data were chosen for TraCE-21K. He (2011) derived the meltwater forcing based on the records of sea level rise (Clark et al., 2002; Peltier, 2004) and geological indicators of ice sheet retreat and meltwater discharge (Licciardi et al., 1999; Clark et al., 2001, 2002; Clark and Mix, 2002; Carlson, 2009; Carlson et al., 2012; Obbink et al., 2010). The rates of meltwater discharge in the model are shown in Fig. 1.

In TraCE-21K, MWP-1A is prescribed from 14.35 to 13.85 ka leading to the abrupt inversion within the BA period: the Older Dryas event (Stanford et al., 2006; Liu et al., 2009). However, this timing may be late according to recent findings that constrain MWP-1A between 14.65 and 14.31 ka (Deschamps et al., 2012), making it simultaneous with the Bolling warming, although the causality relations are still under debate.

The meridional heat transport through a section of the Atlantic basin was calculated as in Bryan (1962):

$$Q_t = \iint c_p \rho \theta v \, \mathrm{d}x \mathrm{d}z \tag{1}$$

Where Q_t is the meridional heat transport, c_p is the sensible heat of seawater, ρ is seawater density, v is the meridional velocity and θ is the potential temperature. The meridional salt transport was calculated in the same way, simply substituting $c_p\theta$ by S, where S is the salinity of seawater.

Here, we define the NADW as being a tongue-like signal of maximum salinity around 2500 m depth in vertical profiles across all longitudes spanning the Atlantic basin extending from the northern high latitudes into the Southern Ocean. The thermohaline signature of NADW was analyzed for the South Atlantic (0–30° S), where this water mass is well defined.

Full Screen / Esc

Printer-friendly Version

Interactive Discussion

3   Results and discussion

The ocean model results are examined with respect to the AMOC through meridional heat and salt transport time series. In contrast with the other oceans, where the heat is generally transported from the equator to the poles, the meridional heat transport in the

5 South Atlantic is directed northward. This happens because the upper branch of the AMOC carries warm surface layer waters northward to compensate the great amount of heat loss in the Nordic Seas thus making the South Atlantic circulation studies instrumental to fully understand Earth's climate system. The heat transport anomaly (with respect to the mean) for the South Atlantic (0–30° S) is shown in Fig. 2 (purple line).

10 It oscillates around the mean of +0.23 PW. Since positive values indicate northward transport, positive anomalies coincide with warm periods in the Northern Hemisphere. A sharp increase of the northward heat transport at ∼ 14.7 ka (which resulted in the Bolling-Allerod (BA) warming in the north Liu et al., 2009) is evident.

Negative meridional heat transport anomalies are associated with the Northern

15 Hemisphere cooling relative to the Heinrich 1 (H1) and Younger Dryas (YD) events, while temperature increases in the Southern Hemisphere as in Liu et al. (2009). After 11 ka, the heat transport values increase slowly towards the mean. From 11 ka to 0 ka, the northward heat transport experiences a long period with little variability. After the mid-Holocene (∼ 6 ka) there is a noticeable stable equilibrium in the heat trans-

20 port between Northern and Southern Hemisphere, at the same time that the meltwater pulses are shutdown in the simulation. The relationship between TraCE-21K meridional heat transport with the meridional salt transport anomalies (where the mean is $-7.58 \times 106 \, \mathrm{kg \, s^{-1}}$) (Fig. 2, green line) shows an out-of-phase behaviour between the two time series. This is best observed through the dispersion diagram in Fig. 3. It shows

25 that the correlations between heat and salt transport are high before and after the BA warming period (circles with a correlation coefficient (r) of −0.99, and triangles with $r = -0.93$, respectively). During the transition (from approximately 14.7 ka to 12.9 ka) the correlation falls (but is still significant; Fig. 3, crosses with $r = -0.79$).

The different slopes of the circles and triangles clusters in Fig. 3 indicate that, overall, the transport exhibit two regimes: a large heat transport and small salt transport before BA and a small heat transport and large salt transport especially after YD (greenish to reddish tones). It is interesting to notice that heat transport is higher at LGM than at modern times, although the temperatures today are far superior than the glacial ones. This strengthens the hypothesis that the AMOC was stronger at 21 ka (Shin et al., 2003; Clauzet et al., 2007), which would explain the large quantity of heat being transported northward. Salt transport, on the other hand, was only consistently positive after the YD period. At glacial times the source of salt for the Atlantic was the salty AABW spanning almost the entire basin from its formation region up to high latitudes of the northern hemisphere. Figures 2 and 3 suggest that northern sources of salty water masses should appear after the YD. The mean potential temperature (θ) vs. salinity (S) for the TraCE-21K model results is shown in Fig. 4a averaged between 30° S and 0° from the LGM (blue dots) to 0 ka (red dots). It can be observed that there is a shift of the curve towards lower salinities throughout the entire water column, which is expected given all the freshwater entering the Atlantic Ocean in the last 21 000 yr. Not so obvious, however, are the changes in the shape of the θ–S curve for the different periods: the θ–S curve at 21 ka is representing only two deep water masses, while the modern curve (0 ka) presents the three main Atlantic Ocean deep water masses (AAIW, NADW and AABW, as indicated in Fig. 4a). The water type that specifies the NADW characteristics (salinity maximum at ∼ 2500 m) does not appear until the early Holocene.

The absence of the NADW during the glacial period is consistent with proxy records (Adkins et al., 2002). θ–S plots considering the same latitudinal interval for the South Atlantic, averaged for 21, 15, 14.1, 13 and 0 ka (before, during and after the MPW-1A) are shown in Fig. 4b. It is clear that the deep salinity maximum characteristic of the NADW within the South Atlantic starts to develop only after MWP-1A (θ–S diagram at 13 ka, pink curve). These changes become evident when examining the vertical profiles of salinity along the Atlantic Ocean for the different climatic periods (Fig. 5). The NADW-like water mass tongue with high salinity values appears only from 11 ka around 2000

m depth (Fig. 5f–g). Before MWP-1A, the water column was strongly stratified below 1500 m (Fig. 5a–c).

Figure 5 shows that the vertical salinity changes are not homogeneous. The impact of the freshwater discharge associated with the simulated MWP-1A does not only impact in reducing the entire water column salinity but also changes the water mass configurations along the Atlantic Ocean. At the LGM the deep ocean was very salty (Fig. 5a) when massive volumes of freshwater were stored in the ice sheets. At the LGM there was increased sea ice formation and associated brine rejection in the Southern Ocean (Shin et al., 2003). The sea ice formation was intensified largely by the lower atmospheric CO_2 concentration (Liu and Milliman, 2004). As a result, the glacial Atlantic Ocean was much more stratified than today (Adkins et al., 2002; Zhang et al., 2012). At about 19 ka, instability of northern ice sheets led to an abrupt discharge of icebergs in the North Atlantic, which is the signature of the H1 event (Denton et al., 2010). During this event, the meltwater input associated with icebergs led to a weaker convection in the north (He et al., 2013) and the total ocean heat transport to north is diminished (as shown in Fig. 2) consistent with Seidov et al. (2001). The main consequences are a decrease in air temperature in the NH and a rise in the SH (Fig. 1 in Liu et al., 2009) which is referred to as the bipolar seesaw. A freshening between ∼ 500–2500 m in the water column (Fig. 5b) is also observed.

When the H1 meltwater discharge was interrupted, the North Atlantic circulation was reinforced. The resulting strengthening of the AMOC and its overshoot possibly triggered the BA abrupt warming in the north at about 14.7 ka (Liu et al., 2009), represented by the abrupt increase of the heat transport anomaly as shown in Fig. 2 (purple line). The model MWP-1A (largest peak in Fig. 1) occurs mostly in the Southern Ocean between 14.35 and 13.85 ka. A freshwater source in the Southern Ocean will generate a salinity anomaly throughout the entire water column that will spread to all other ocean basins (Stouffer et al., 2007) mostly in the bottom layers. This can be observed in Fig. 5c–d. We also see in Fig. 5d a high salinity region centered at 30° N confined within the upper layers. This is what is thought here as the precursor of the NADW

water type source. The water in this high salinity pocket has relative high tempera-
tures (not shown), which maintains its density lower than that necessary for sinking.
As a result, the formation of the deep water in the North Atlantic is not observed.
The intrusion of freshwater in the North Atlantic during Heinrich 0 at Younger Dryas
(around 12 ka) makes the salty pocket disappear through mixing at the same time that
the salinity anomaly that originated from the freshwater input from the southern source
for the model MWP-1A continues to spread over the Atlantic basin (Fig. 5e). As soon
as the meltwater discharge from the North Atlantic is interrupted around 11.7 ka, the
heat transport towards the north is re-established. At this time, the high salinity pocket
centered around 30° N ($\sim$ 500 m) reappears in the vertical profile (Fig. 5f). The South-
ern Ocean deep and bottom waters at this moment are much fresher than at 13 ka
due to mixing of MWP-1A discharge throughout the water column. The salinity barrier,
which was responsible for the high stratification, is eroded and the dense water that
was confined to the surface layers can finally sink. This is when the features of the
modern NADW first appear in the deep ocean since the LGM (salty tongue at Fig. 5f)
marking the birth of NADW as we know it today. We can compare this same structure
with the one presented in Fig. 5g, which stands for 0 ka (1950). Also, Fig. 5g shows
that the model succeeded in representing the three main modern water masses that
are observed in the profile obtained with observed data from the World Ocean Circu-
lation Experiment (WOCE) seen in Fig. 5h. The differences between the two profiles
(Fig. 5g and h) can be explained by the low spatial resolution of the model.

The TraCE-21 model results are consistent with the idea of a weaker NADW during
YD, discussed by several studies based on proxy-data (Boyle, 1987; Hughen et al.,
1998; McManus et al., 2004; Piotrowski et al., 2005; Praetorius et al., 2008; Roberts
et al., 2010). Furthermore, through ^{231}Pa/^{230}Th ratio analysis, Negre et al. (2010) dis-
cuss that the modern Atlantic circulation was only established during the Holocene,
which is also consistent with the evolution of the salinity-based water mass structure
presented in Fig. 5. The establishment of the NADW as the main southward component
of the AMOC preceded the change in the overturning circulation geometry. The AMOC

Title Page

Abstract | Introduction

Conclusions | References

Tables | Figures

|◄ | ►|

◄ | ►

Back | Close

Full Screen / Esc

Printer-friendly Version

Interactive Discussion

Full Screen / Esc

Printer-friendly Version

Interactive Discussion

became deeper (Lippold et al., 2012), meridional heat transport became more stable and the NADW becomes the main salt exporter across the Atlantic Ocean. Hence, the steep triangle cluster on Fig. 3 is explained: a smaller variability on the heat transport northwards and larger salt transport southwards in the Holocene.

4 Conclusions

This study examines the evolution of the South Atlantic Ocean salinity distribution relative to the NADW since the LGM, considering several meltwater pulses recorded in sea-level proxy data, through the analysis of the results of the first transient paleoclimate numerical simulation from the LGM to Present Day (PD). After evaluating the water mass distribution in the South Atlantic Ocean, it is concluded that the NADW, as we know today, was established at the onset of the Holocene (i.e. 11 ka), playing an important role on the heat and salt transport stabilization during that period. Results show a salinity barrier generated at the LGM by Southern Ocean deep salty waters that prevents the deep NADW formation in its Northern Hemisphere origin. Zhang et al. (2012) discussed the importance of this stratification relative to the spatial configuration and strength of the AMOC.

Therefore, much of the PD structure of the NADW occurs because of the impact of the freshwater discharge associated with the timing of the MWP-1A, which in this model is predominantly of Southern Ocean origin. This geographical source guarantees that the freshwater released spreads over the global ocean unlike the meltwater pulses from the North Atlantic, which are mostly constrained around their source region (Stouffer et al., 2007). In other words, if MWP-1A had occurred only within the northern ice sheets the resulting freshening would occur mostly at the surface, which hinders the NADW formation process. Furthermore, it is important to remember that these conclusions apply for the period starting at LGM, which means that a similar form of the PD NADW could have existed before. Using isotopic analysis, Frank et al. (2002) showed

that a water mass of NH origin was present in the Southern Ocean between 14 and 3 millions of years ago, but was progressively reduced since then.

Other studies point out that the source of Antarctic meltwater at ~ 14 ka could be from the western side of the continental ice sheet (Weaver et al., 2003; Deschamps et al., 2012). Today, trends of reduced ice cover have been observed at the same location (Thomas et al., 2004; Jacobs et al., 2011; Joughin and Alley, 2011). Could this ice sheet melting change NADW properties again in the future?

References

Adkins, J. F., McIntyre, K., and Schrag, D. P.: The salinity, temperature, and δ18O of the glacial deep ocean, Science, 298, 1769–1773, 2002. 6381, 6382

Alley, R. B.: The Younger Dryas cold interval as viewed from central Greenland, Quaternary Sci. Rev., 19, 213–226, 2000. 6378

Anderson, J. B., Kirshner, A. E., and Simms, A. R.: Constraints on Antarctic Ice Sheet configuration during and following the last glacial maximum and its episodic contribution to sea-level rise, Special Publications, 381, Geological Society, London, doi:10.1016/S0277-3791(01)00083-X, 2013. 6377

Bassett, S. E., Milne, G. A., Mitrovica, J. X., and Clark, P. U.: Ice sheet and solid earth influences on far-field sea-level histories, Science, 309, 925–928, 2005. 6377

Bassett, S., Milne, G., Bentley, M., and Huybrechts, P.: Modelling Antarctic sea-level data to explore the possibility of a dominant Antarctic contribution to meltwater pulse IA, Quaternary Sci. Rev., 26, 2113–2127, 2007. 6377

Bentley, M. J., Fogwill, C. J., Le Brocq, A. M., Hubbard, A. L., Sugden, D. E., Dunai, T. J., and Freeman, S. P.: Deglacial history of the West Antarctic Ice Sheet in the Weddell Sea embayment: constraints on past ice volume change, Geology, 38, 411–414, 2010. 6377

Full Screen / Esc

Printer-friendly Version

Interactive Discussion

Bethke, I., Li, C., and Nisancioglu, K. H.: Can we use ice sheet reconstructions to constrain meltwater for deglacial simulations?, Paleoceanography, 27, PA2205, doi:10.1029/2011PA002258, 2012. 6377

Boyle, E. A.: North Atlantic thermohaline circulation during the past 20,000 years linked to high-latitude surface temperature, Nature, 330, 35–40, doi:10.1038/330035a0, 1987. 6383

Boyle, E. and Leach, H.: Last-glacial-maximum North Atlantic deep water: on, off or somewhere in-between? [and discussion], Philos. T. R. Soc. Lon. B, 348, 243–253, 1995. 6378

Bryan, K.: Measurements of meridional heat transport by ocean currents, J. Geophys. Res., 67, 3403–3414, 1962. 6379

Carlson, A. E.: Geochemical constraints on the Laurentide Ice Sheet contribution to meltwater pulse 1A, Quaternary Sci. Rev., 28, 1625–1630, 2009. 6377, 6379

Carlson, A. E., Ullman, D. J., Anslow, F. S., He, F., Clark, P. U., Liu, Z., and Otto-Bliesner, B. L.: Modeling the surface mass-balance response of the Laurentide Ice Sheet to Bølling warming and its contribution to Meltwater Pulse 1A, Earth Planet. Sc. Lett., 315, 24–29, 2012. 6377, 6379

Clark, P. U. and Mix, A. C.: Ice sheets and sea level of the Last Glacial Maximum, Quaternary Sci. Rev., 21, 1–7, 2002. 6379

Clark, P. U., Alley, R. B., Keigwin, L. D., Licciardi, J. M., Johnsen, S. J., and Wang, H.: Origin of the first global meltwater pulse following the last glacial maximum, Paleoceanography, 11, 563–577, 1996. 6377

Clark, P. U., Marshall, S. J., Clarke, G. K., Hostetler, S. W., Licciardi, J. M., and Teller, J. T.: Freshwater forcing of abrupt climate change during the last glaciation, Science, 293, 283–287, 2001. 6379

Clark, P. U., Mitrovica, J., Milne, G., and Tamisiea, M.: Sea-level fingerprinting as a direct test for the source of global meltwater pulse IA, Science, 295, 2438–2441, 2002. 6377, 6379

Clauzet, G., Wainer, I., Lazar, A., Brady, E., and Otto-Bliesner, B.: A numerical study of the South Atlantic circulation at the Last Glacial Maximum, Palaeogeogr. Palaeocl., 253, 509–528, 2007. 6381

Curry, W. B. and Oppo, D. W.: Glacial water mass geometry and the distribution of $\delta^{13}C$ of ΣCO_2 in the western Atlantic Ocean, Paleoceanography, 20, PA1017, doi:10.1029/2004PA001021, 2005. 6377, 6378

Denton, G., Anderson, R., Toggweiler, J., Edwards, R., Schaefer, J., and Putnam, A.: The last glacial termination, Science, 328, 1652–1656, 2010. 6382

Deschamps, P., Durand, N., Bard, E., Hamelin, B., Camoin, G., Thomas, A. L., Hender-
son, G. M., Okuno, J., and Yokoyama, Y.: Ice-sheet collapse and sea-level rise at the Bolling
warming 14 600 years ago, Nature, 483, 559–564, 2012. 6376, 6377, 6379, 6385

Duplessy, J., Shackleton, N., Fairbanks, R., Labeyrie, L., Oppo, D., and Kallel, N.: Deepwater
source variations during the last climatic cycle and their impact on the global deepwater
circulation, Paleoceanography, 3, 343–360, doi:10.1029/PA003i003p00343, 1988. 6378

Fairbanks, R. G.: A 17 000 year glacio-eustatic sea level record: influence of glacial melting
rates on the Younger Dryas event and deep-ocean circulation, Nature, 342, 637–642, 1989.
6376, 6377

Frank, M., Whiteley, N., Kasten, S., Hein, J. R., and O'Nions, K.: North Atlantic Deep Water
export to the Southern Ocean over the past 14 Myr: evidence from Nd and Pb isotopes in
ferromanganese crusts, Paleoceanography, 17, 12 pp., doi:10.1029/2000PA000606, 2002.
6384

Gregoire, L. J., Payne, A. J., and Valdes, P. J.: Deglacial rapid sea level rises caused by ice-
sheet saddle collapses, Nature, 487, 219–222, 2012. 6377

Hanebuth, T., Stattegger, K., and Bojanowski, A.: Termination of the Last Glacial Maximum
sea-level lowstand: the Sunda-Shelf data revisited, Global Planet. Change, 66, 76–84, 2009.
6376

He, F.: Simulating transient climate evolution of the last deglaciation with CCSM3, Ph.D. thesis,
University of Wisconsin-Madison, Madison, WI, 2011. 6378, 6379, 6391

He, F., Shakun, J. D., Clark, P. U., Carlson, A. E., Liu, Z., Otto-Bliesner, B. L., and
Kutzbach, J. E.: Northern Hemisphere forcing of Southern Hemisphere climate during the
last deglaciation, Nature, 494, 81–85, 2013. 6382

Hughen, K. A., Overpeck, J. T., Lehman, S. J., Kashgarian, M., Southon, J., Peterson, L. C.,
Alley, R., and Sigman, D. M.: Deglacial changes in ocean circulation from an extended radio-
carbon calibration, Nature, 391, 65–68, 1998. 6378, 6383

Jacobs, S. S., Jenkins, A., Giulivi, C. F., and Dutrieux, P.: Stronger ocean circulation and in-
creased melting under Pine Island Glacier ice shelf, Nat. Geosci., 4, 519–523, 2011. 6385

Joos, F. and Spahni, R.: Rates of change in natural and anthropogenic radiative forcing over
the past 20 000 years, P. Natl. Acad. Sci. USA, 105, 1425–1430, 2008. 6379

Joughin, I. and Alley, R. B.: Stability of the West Antarctic ice sheet in a warming world, Nat.
Geosci., 4, 506–513, 2011. 6385

Jouzel, J., Vaikmae, R., Petit, J., Martin, M., Duclos, Y., Stievenard, M., Lorius, C., Toots, M., Melieres, M., Burckle, L., Barkov, N., and Kotlyakov, V.: The two-step shape and timing of the last deglaciation in Antarctica, Clim. Dynam., 11, 151–161, doi:10.1007/BF00223498, 1995. 6378

5 Kienast, M., Hanebuth, T. J., Pelejero, C., and Steinke, S.: Synchroneity of meltwater pulse 1a and the Bølling warming: new evidence from the South China Sea, Geology, 31, 67–70, 2003. 6377

Licciardi, J. M., Teller, J. T., and Clark, P. U.: Freshwater routing by the Laurentide Ice Sheet during the last deglaciation, in: Mechanisms of Global Climate Change at Millennial Time

10 Scales, 177–201, doi:10.1029/GM112p0177, American Geophysical Union, Washington, D. C., 1999. 6379

Lippold, J., Luo, Y., Francois, R., Allen, S. E., Gherardi, J., Pichat, S., Hickey, B., and Schulz, H.: Strength and geometry of the glacial Atlantic Meridional Overturning Circulation, Nat. Geosci., 5, 813–816, doi:10.1038/ngeo1608, 2012. 6377, 6384

15 Liu, J. P. and Milliman, J. D.: Reconsidering melt-water pulses 1A and 1B: global impacts of rapid sea-level rise, Journal of Ocean University of China, 3, 183–190, doi:10.1007/s11802-004-0033-8, 2004. 6382

Liu, Z., Otto-Bliesner, B., He, F., Brady, E., Tomas, R., Clark, P., Carlson, A., Lynch-Stieglitz, J., Curry, W., Brook, E., Erickson, D., Jacob, R., Kutzbach, J., and Cheng, J.: Transient simu-

20 lation of last deglaciation with a new mechanism for Bølling-Allerød warming, Science, 325, 310–314, 2009. 6378, 6379, 6380, 6382

Lynch-Stieglitz, J., Curry, W. B., Oppo, D. W., Ninneman, U. S., Charles, C. D., and Munson, J.: Meridional overturning circulation in the South Atlantic at the last glacial maximum, Geochem. Geophy. Geosy., 7, Q10N03, doi:10.1029/2005GC001226, 2006. 6378

25 Mackintosh, A., Golledge, N., Domack, E., Dunbar, R., Leventer, A., White, D., Pollard, D., DeConto, R., Fink, D., Zwartz, D., Gore, D., and Lavoie, C.: Retreat of the East Antarctic ice sheet during the last glacial termination, Nat. Geosci., 4, 195–202, 2011. 6377

Marchitto, T. M. and Broecker, W. S.: Deep water mass geometry in the glacial Atlantic Ocean: a review of constraints from the paleonutrient proxy Cd/Ca, Geochem. Geophy. Geosy., 7,

30 Q12003, doi:10.1029/2006GC001323, 2006. 6378

Marchitto, T. M., Oppo, D. W., and Curry, W. B.: Paired benthic foraminiferal Cd/Ca and Zn/Ca evidence for a greatly increased presence of Southern Ocean Water in the glacial North Atlantic, Paleoceanography, 17, 10–1, doi:10.1029/2000PA000598, 2002. 6377

McManus, J., Francois, R., Gherardi, J.-M., Keigwin, L., and Brown-Leger, S.: Collapse and rapid resumption of Atlantic meridional circulation linked to deglacial climate changes, Nature, 428, 834–837, 2004. 6377, 6383

Negre, C., Zahn, R., Thomas, A. L., Masqué, P., Henderson, G. M., Martínez-Méndez, G., Hall, I. R., and Mas, J. L.: Reversed flow of Atlantic deep water during the Last Glacial Maximum, Nature, 468, 84–88, 2010. 6383

Obbink, E. A., Carlson, A. E., and Klinkhammer, G. P.: Eastern North American freshwater discharge during the Bølling-Allerød warm periods, Geology, 38, 171–174, 2010. 6379

Otto-Bliesner, B. L., Brady, E. C., Clauzet, G., Tomas, R., Levis, S., and Kothavala, Z.: Last glacial maximum and Holocene climate in CCSM3, J. Climate, 19, 2526–2544, doi:10.1175/JCLI3748.1, 2006. 6378

Peltier, W. R.: Ice age paleotopography, Science, 265, 195–195, 1994. 6377

Peltier, W.: Global glacial isostasy and the surface of the ice-age Earth: the ICE-5G (VM2) model and GRACE, Annu. Rev. Earth Planet. Sci., 32, 111–149, doi:10.1146/annurev.earth.32.082503.144359, 2004. 6379

Peltier, W.: On the hemispheric origins of meltwater pulse 1a, Quaternary Sci. Rev., 24, 1655–1671, 2005. 6377

Peltier, W. and Fairbanks, R. G.: Global glacial ice volume and Last Glacial Maximum duration from an extended Barbados sea level record, Quaternary Sci. Rev., 25, 3322–3337, 2006. 6376, 6377

Piotrowski, A. M., Goldstein, S. L., Hemming, S. R., and Fairbanks, R. G.: Temporal relationships of carbon cycling and ocean circulation at glacial boundaries, Science, 307, 1933–1938, 2005. 6383

Praetorius, S. K., McManus, J. F., Oppo, D. W., and Curry, W. B.: Episodic reductions in bottom-water currents since the last ice age, Nat. Geosci., 1, 449–452, 2008. 6377, 6383

Roberts, N. L., Piotrowski, A. M., McManus, J. F., and Keigwin, L. D.: Synchronous deglacial overturning and water mass source changes, Science, 327, 75–78, 2010. 6383

Seidov, D., Barron, E., and Haupt, B. J.: Meltwater and the global ocean conveyor: northern versus southern connections, Global Planet. Change, 30, 257–270, 2001. 6377, 6382

Shin, S.-I., Liu, Z., Otto-Bliesner, B., Brady, E., Kutzbach, J., and Harrison, S.: A simulation of the Last Glacial Maximum climate using the NCAR-CCSM, Clim. Dynam., 20, 127–151, doi:10.1007/s00382-002-0260-x, 2003. 6381, 6382

Stanford, J. D., Rohling, E. J., Hunter, S. E., Roberts, A. P., Rasmussen, S. O., Bard, E., Mc-Manus, J., and Fairbanks, R. G.: Timing of meltwater pulse 1a and climate responses to meltwater injections, Paleoceanography, 21, PA4103, doi:10.1029/2006PA001340, 2006. 6377, 6379

Stenni, B., Masson-Delmotte, V., Selmo, E., Oerter, H., Meyer, H., Röthlisberger, R., Jouzel, J., Cattani, O., Falourd, S., Fischer, H., Hoffmann, G., Iacumin, P., Johnsen, S., Minster, B., and Udisti, R.: The deuterium excess records of EPICA Dome C and Dronning Maud Land ice cores (East Antarctica), Quaternary Sci. Rev., 29, 146–159, 2010. 6377

Stouffer, R. J., Seidov, D., and Haupt, B. J.: Climate response to external sources of freshwater: North Atlantic versus the Southern Ocean, J. Climate, 20, 436–448, doi:10.1175/JCLI4015.1, 2007. 6382, 6384

Thomas, R., Rignot, E., Casassa, G., Kanagaratnam, P., Acuña, C., Akins, T., Brecher, H., Frederick, E., Gogineni, P., Krabill, W., Manizade, S., Ramamoorthy, H., Rivera, A., Russel, R., Sonntag, J., Swift, R., Yungel, J., and Zwally, J.: Accelerated sea-level rise from West Antarctica, Science, 306, 255–258, 2004. 6385

Weaver, A. J., Saenko, O. A., Clark, P. U., and Mitrovica, J. X.: Meltwater pulse 1A from Antarctica as a trigger of the Bølling-Allerød warm interval, Science, 299, 1709–1713, 2003. 6376, 6377, 6378, 6385

Yu, E.-F., Francois, R., and Bacon, M. P.: Similar rates of modern and last-glacial ocean thermohaline circulation inferred, Nature, 379, 689–694, doi:10.1038/379689a0, 1996. 6378

Zhang, X., Lohmann, G., Knorr, G., and Xu, X.: Different ocean states and transient characteristics in Last Glacial Maximum simulations and implications for deglaciation, Clim. Past, 9, 2319–2333, doi:10.5194/cp-9-2319-2013, 2013. 6377, 6382, 6384
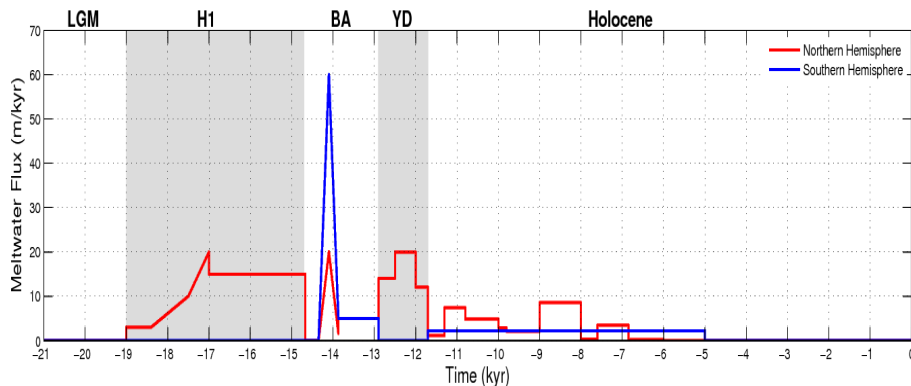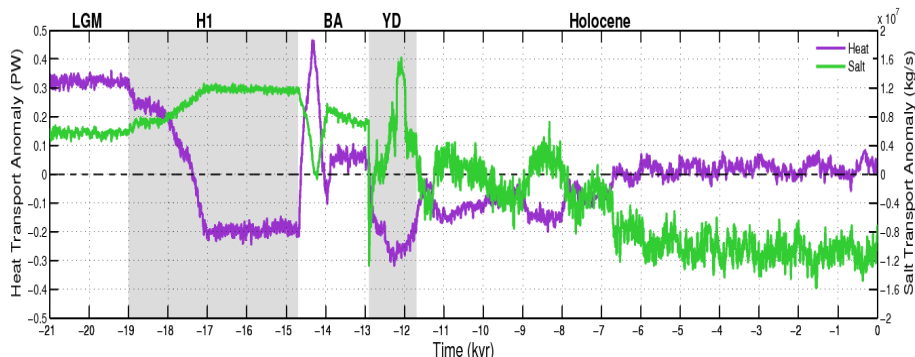
Fig. 1. Meltwater discharges from the Northern (red line) and Southern (blue line) Hemisphere ($1\,\mathrm{m\,kyr^{-1}} = 1\,\mathrm{m}$ of equivalent global sea level rise per thousand year $= 0.0115\,\mathrm{Sv}$) (He, 2011). The shaded areas represent the main climatic events in the last deglaciation: Last Glacial Maximum (LGM), Heinrich event 1 (H1), Bolling-Allerod (BA), Younger Dryas (YD) and Holocene.

Fig. 2. TraCE-21K meridional heat (purple line) and salt (green line) transport anomaly between 30° S and 0°. Positive values denote northward transport. The shaded areas represent the main climatic events in the last deglaciation: Last Glacial Maximum (LGM), Heinrich event 1 (H1), Bolling-Allerod (BA), Younger Dryas (YD) and Holocene.
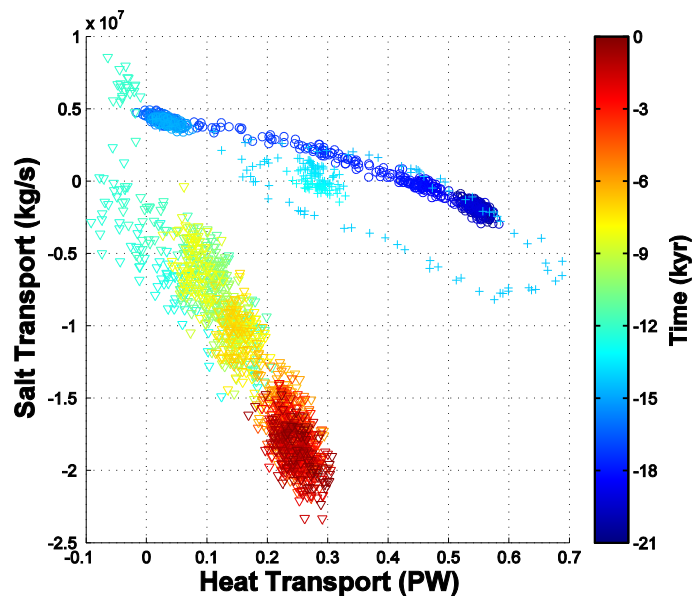
Fig. 3. Dispersion diagram showing negative correlation between heat and salt transport in South Atlantic (30° S–0°). The circles represent data for the period that precede Bolling-Allerod; the crosses stand for the BA period; and the triangles show data from Younger Dryas on. The colors stand for time evolution, according to the colorbar on the right.
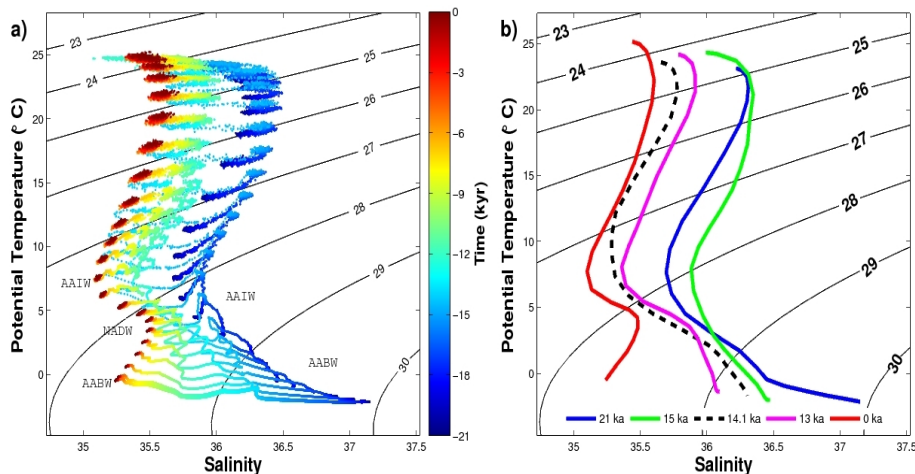
Fig. 4. TraCE-21K–θS diagram averaged between 0° to 30°S, at 25°W. **(a)** Time evolution is represented by the color range. The acronyms indicate the main water masses: AAIW – Antarctic Intermediate Water; AABW – Antarctic Bottom Water; NADW – North Atlantic Deep Water. **(b)** θ–S diagram averaged for the key climatic periods considered in this study: LGM (blue), before (green), during (dashed black) and after (pink) MWP-1A, and 0 ka (red).
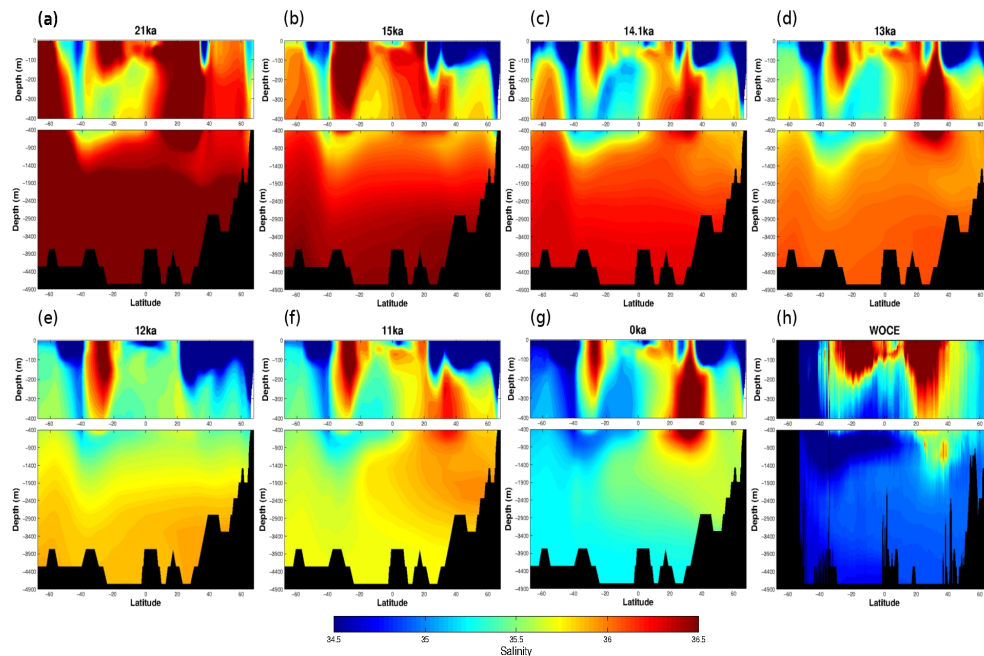
Fig. 5. TraCE-21K salinity meridional sections across the Atlantic Ocean (25° W) at **(a)** 21 ka, **(b)** 15 ka, **(c)** 14.1 ka, **(d)** 13 ka, **(e)** 12 ka, **(f)** 11 ka and **(g)** 0 ka; **(h)** transect across the Atlantic Ocean with WOCE data.